JOURNAL OF MATERIALS SCIENCE 32 (1997) 2037–2043

The tensile strength of short fibre-reinforced composites

Y. T. ZHU, W. R. BLUMENTHAL, T. C. LOWE
MST-5, Mail Stop G755, Materials Science and Technology Division, Los Alamos National Laboratory, Los Alamos, NM 87545, USA

Tensile strength is one of the most important mechanical properties of structural short fibre composites, and its prediction is essential for composite design. This paper develops a strength theory for three-dimensionally oriented short fibre-reinforced composites. The contribution of direct fibre strengthening to the composite strength is derived using a maximum-load composite failure criterion. Other strengthening mechanisms, such as residual thermal stress, matrix work hardening and short fibre dispersion hardening are also incorporated into the calculation of composite strength. In the derivation of direct fibre strengthening, the strain and stress of short fibres with different inclination angles were first derived, and the direct fibre strengthening was calculated from the maximum total load these short fibres can carry in the composite loading direction.

1. Introduction

Short fibre composites have found extensive application in automobiles, sporting goods and cutting tools [1, 2]. The strength of these composites is one of their most important properties, and its prediction is essential in the design of composite parts. Although successful theories have been developed to predict the strength of composites having continuous or discontinuous fibres with unidirectional orientation [3–7], the strength of three-dimensionally oriented short fibre composites has not been well studied. The models of Chen [8] and Halpin and Kardos [9] are among the earliest works on the strength of short fibre-reinforced composites. They approximated the composite as a stack of unidirectional short fibre-reinforced laminae bonded together at different angles, which does not represent the real situation. In addition, these two theories do not provide any clear relationship between the composite strength and the properties of its constituents, because they rely on the experimental failure strength and strain data of the unidirectional laminae. Friend [10, 11] proposed an empirical strength equation for randomly-oriented short fibre-reinforced metal matrix composites. Owing to its empirical nature, his equation can only be used in particular alloy matrix composites. For example, it seems to agree with experimental data for some aluminium alloy matrix composites, but it cannot explain the high strength of composites with a pure aluminium matrix.

Fukuda *et al.* [12] were the first to develop a theory to predict the strength of composites reinforced with short fibres oriented randomly, or otherwise, in three dimensions. However, their theory under-predicts the contribution of the fibres to the composite strength and does not fit experimentally observed composite strength data. Zhu *et al.* [13, 14] developed theories to predict the strength of composites reinforced with randomly-oriented short fibres. But, the random orientation of short fibres is an idealized situation, which can seldom be obtained during the fabrication of real short fibre composites [15]. To predict the strength of a real short fibre composite, the distribution of fibre orientation has to be taken into account. The three-dimensional fibre-orientation distribution can be obtained using image analysis or optical diffraction methods [16–18], and this makes it possible to assess the strength of a real short fibre composite.

The objective of this work was to develop a strength theory for composites reinforced with three-dimensionally oriented short fibres. In this theory, the maximum total load is adopted as the composite failure criterion. Special cases, such as the strengths of composites reinforced with unidirectionally-oriented short fibres, with two-dimensional randomly-oriented short fibres, and with three-dimensional randomly-oriented short fibres, are also presented.

2. Strength theory

The strengthening mechanisms in short fibre-reinforced metal- and polymer-matrix composites include several or all of the following: direct short fibre strengthening [13], residual thermal stress in fibres [19, 20], and matrix work hardening induced by short fibre dispersion [13] and by thermal stress-induced dislocations [19–23]. Direct short fibre strengthening is the most significant strengthening mechanism and, therefore, will be examined first.

2.1. Direct fibre strengthening

The following two assumptions are made for simplicity: (1) all fibres in a composite have the same tensile

0022–2461

strength, and (2) perfect bonding exists between fibres and the matrix. The first assumption is commonly used in theories of composite strength and is quite reasonably adopted in this work.

Fibres with smaller inclination angles from the loading direction (see Fig. 1) bear larger stresses and break first during tensile loading. Because the fibre usually has higher Young's modulus than the matrix, these broken short fibres shift their previously carried load through the matrix to fibres with larger inclination angles, which have not yet reached their ultimate strength. Assuming that θ_0 is the critical inclination angle within which every fibre is broken, i.e. fibres with the inclination angle θ_0 bear a stress equal to their ultimate strength and are just about to break, the total load carried by the remaining short fibres can be calculated by integrating the load contributions by all these fibres. The total load is a function of θ_0 and can be expressed as $P(\theta_0)$. The maximum of $P(\theta_0)$ can be considered as the total load that the short fibres carry at composite failure and can be used to calculate the direct fibre strengthening.

Before deriving $P(\theta_0)$, we need first to calculate the load carried by a fibre with an inclination angle, θ. Shown in Fig. 1 is a fibre with an inclination angle $0 \leq \theta \leq \pi/2$ in a composite sample. For simplicity, we will assume an isotropic Poisson's ratio, ν, for the composite. Under a total load, P, along the x_3 direction, the composite strain, ε_c, is produced in the loading direction

$$\varepsilon_c = \varepsilon_{33} \tag{1}$$

and strains in x_1 and x_2 directions can be calculated as

$$\varepsilon_{11} = \varepsilon_{22} = -\nu\varepsilon_{33}. \tag{2}$$

To calculate the strain in a fibre with an inclination angle θ, let us rotate the coordination system around the x_1 axis clockwise by an angle of θ (see Fig. 1). The transformation matrix A is

$$A = \begin{bmatrix} a_{11} & a_{12} & a_{13} \\ a_{21} & a_{22} & a_{23} \\ a_{31} & a_{32} & a_{33} \end{bmatrix} = \begin{bmatrix} 1 & 0 & 0 \\ 0 & \cos\theta & -\sin\theta \\ 0 & \sin\theta & \cos\theta \end{bmatrix} \tag{3}$$

where $a_{ij} = \cos\alpha_{ij}$, and α_{ij} is the angle between y_i and x_j. The strain in the y_3 direction (along the fibre) can be calculated as

$$\varepsilon^y_{33}(\theta) = \sum_{i=1}^{3} a_{3i} \sum_{j=1}^{3} a_{3j}\varepsilon_{ij} = \varepsilon_{33}(\cos^2\theta - \nu\sin^2\theta) \tag{4}$$

Substituting Equation 1 into Equation 4 yields

$$\varepsilon^y_{33}(\theta) = \varepsilon_c(\cos^2\theta - \nu\sin^2\theta) \tag{5}$$

By the definition of the critical inclination angle θ_0, fibres with θ_0 will be at their failure strain and stress, therefore

$$\varepsilon^y_{33}(\theta_0) = \varepsilon_f = \varepsilon_c(\cos^2\theta_0 - \nu\sin^2\theta_0) \tag{6}$$

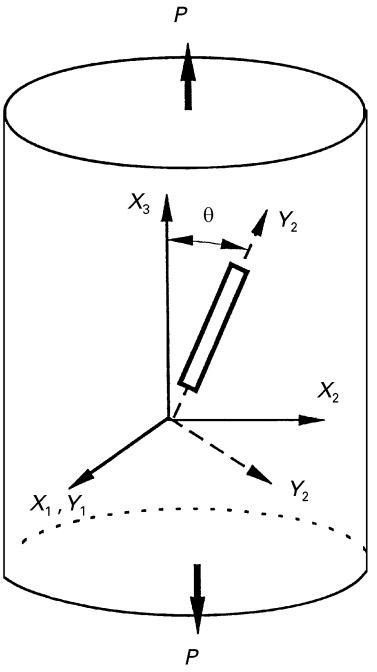

Figure 1 Definition of off-axis angle, θ.

where ε_f is the fibre failure strain. Substituting Equation 6 into Equation 5 yields

$$\varepsilon^y_{33}(\theta) = \frac{\varepsilon_f(\cos^2\theta - \nu\sin^2\theta)}{\cos^2\theta_0 - \nu\sin^2\theta_0} \tag{7}$$

At $\theta < \theta_0$, $\varepsilon^y_{33}(\theta)$ calculated with Equation 7 will be larger than ε_f, and so the fibre is broken and can no longer carry load, i.e. the stress in a fibre with an inclination angle $\theta < \theta_0$ is

$$\sigma(\theta) = 0 \tag{8}$$

The strain in fibres with $\theta \geq \theta_0$ can be considered equal to $\varepsilon^y_{33}(\theta)$; and the stress in these fibres, therefore, is

$$\sigma(\theta) = E_f\varepsilon^y_{33}(\theta) \tag{9}$$

where E_f is the Young's modulus of the fibre. Considering $\sigma_f = E_f\varepsilon_f$, where σ_f is the fibre fracture strength, and substituting Equation 7 into Equation 9, we get

$$\sigma(\theta) = \frac{\sigma_f(\cos^2\theta - \nu\sin^2\theta)}{(\cos^2\theta_0 - \nu\sin^2\theta_0)} \tag{10}$$

Setting $\sigma(\theta) = 0$ in Equation 10 yields

$$\sin^2\theta_f = 1/(1 + \nu) \tag{11}$$

where θ_f can be calculated from Equation 11. From Equation 10, it can be seen that $\sigma(\theta)$ is positive if $\theta < \theta_f$, which means tensile stress in the fibre. But, if θ is larger than θ_f, $\sigma(\theta)$ will be negative due to the Poisson constriction. Because fibres usually have higher Young's modulus than the matrix, fibres should always have higher resistance to elastic deformation than the matrix. Therefore, those fibres under the Poisson constriction will also make a positive contribution towards the composite strength. Based on the above argument, the absolute value of $\sigma(\theta)$ should be

used in the calculation of total load carried by fibres towards the loading direction.

With above discussion, the stress in fibres with different inclination angles can be summarized as

$$\sigma(\theta) = \begin{cases} 0 & \theta < \theta_0 \\ \dfrac{\sigma_f(\cos^2\theta - \nu\sin^2\theta)}{\cos^2\theta_0 - \nu\sin^2\theta_0} & \theta_0 \le \theta < \theta_f \\ -\dfrac{\sigma_f(\cos^2\theta - \nu\sin^2\theta)}{\cos^2\theta_0 - \nu\sin^2\theta_0} & \theta_f \le \theta \le \dfrac{\pi}{2} \end{cases} \quad (12)$$

To obtain the total load, $P(\theta)$, at a specimen cross-section perpendicular to the loading direction (hereafter referred to as cross-section A, as indicated in Fig. 2), the orientation-density distribution of fibres intercepted by the cross-section, $n_c(\theta)$, is also needed. Defining the fibre orientation-density distribution in the volume of the specimen as $n_v(\theta)$, we can obtain $n_c(\theta)$ from $n_v(\theta)$ by taking into account the following two factors: first, the probability of a fibre being intercepted by the cross-section A changes with the inclination angle of the fibre; second, not every fibre intercepted by cross-section A bears load (e.g. when the fibre end is cut). $n_v(\theta)$ can be expressed as

$$n_v(\theta) = Nf(\theta) \quad (13)$$

where N is the total number of short fibres in the composite specimen and $f(\theta)$ is the normalized fibre-orientation distribution, which can be determined using image analysis [16, 17].

To calculate $n_c(\theta)$, it is also necessary to know the effective load-carrying length of a short fibre, which can be expressed as

$$l_e = \bar{l} - 2\delta \quad (14)$$

where $\bar{l}$ is the average fibre length, which also can be obtained from image analysis [17], and δ is the equivalent non load-carrying length at each end of the short fibre. A shear-lag-type analysis by Rosen [24] yields a fibre stress variation near the fibre end as

$$\sigma_{fe}(x) = \sigma_{f0}[1 - \exp(\lambda x)] \quad (15)$$

where x is the distance from the fibre end, σ_{f0} is the stress in the fibre at a large distance from the fibre end, and

$$\lambda = \frac{2}{\bar{d}}\left(\frac{G_m}{E_f}\right)^{1/2}\left(\frac{V_f^{1/2}}{1 - V_f^{1/2}}\right)^{1/2} \quad (16)$$

where $\bar{d}$ is the average fibre diameter, which is known before the fabrication of a composite, or can be determined from image analysis [17], G_m is the shear modulus of the matrix, and V_f is the fibre volume fraction. δ can be calculated from Equation 15 as

$$\delta = \frac{1}{\sigma_{f0}}\int_0^\infty [\sigma_{f0} - \sigma_{fe}(x)]\,dx = \frac{\bar{d}}{2}[(V_f^{-1/2} - 1)E_f/G_m]^{1/2} \quad (17)$$

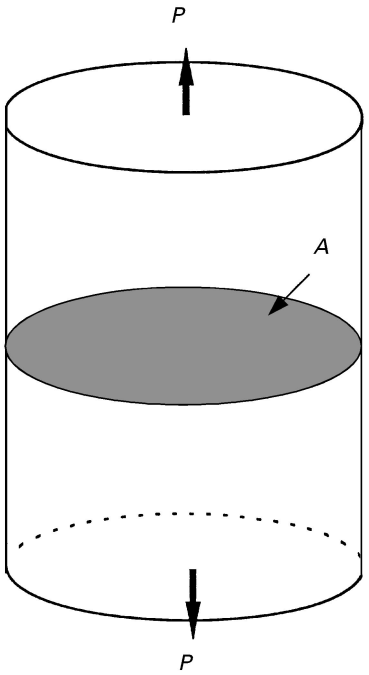

Figure 2 A composite sample and its cross-section.

The projected effective fibre length on the loading direction can be calculated as

$$l_p(\theta) = l_e\cos\theta = [\bar{l} - 2\delta]\cos\theta \quad (18)$$

$n_c(\theta)$ can be calculated from $n_v(\theta)$ and $l_p(\theta)$ as

$$n_c(\theta) = n_v(\theta)l_p(\theta)/L \quad (19)$$

where L is the composite specimen length.

The total number of fibres in a composite specimen, N, can be calculated by the following equation

$$N = \frac{LAV_f}{\bar{l}\bar{a}_f} \quad (20)$$

where A is the sample cross-sectional area and $\bar{a}_f = \pi\bar{d}^2/4$. Substituting Equations 13, 17, 18 and 20 into Equation 19 yields

$$n_c(\theta) = \frac{V_f A}{\bar{a}_f}\left\{1 - \frac{\bar{d}}{\bar{l}}[(V_f^{-1/2} - 1)E_f/G_m]^{1/2}\right\} \times f(\theta)\cos\theta \quad (21)$$

Knowing $n_c(\theta)$, we can calculate $P(\theta_0)$ as

$$P(\theta_0) = \int_{\theta_0}^{\pi/2} n_c(\theta)\sigma(\theta)\bar{a}_f\cos\theta\,d\theta \quad (22)$$

Substituting Equations 12 and 21 into Equation 22 and integrating yields

$$P(\theta_0) = \frac{V_f A\sigma_f\{1 - \bar{d}[(V_f^{-1/2} - 1)E_f/G_m]^{1/2}/\bar{l}\}}{\cos^2\theta_0 - \nu\sin^2\theta_0} \times\left[\int_{\theta_0}^{\theta_f} g(\theta)\,d\theta - \int_{\theta_f}^{\pi/2} g(\theta)\,d\theta\right] \quad (23)$$

where

$$g(\theta) = f(\theta)(\cos^2\theta - \nu\sin^2\theta)\cos^2\theta \quad (24)$$

The direct short fibre strengthening can be calculated as

$$\sigma_c^f = \frac{[P(\theta_0)]_{max}}{A} = V_f\sigma_f\left\{1-\frac{\bar{d}}{\bar{l}}[(V_f^{-1/2}-1)E_f/G_m]^{1/2}\right\} \times \left[\frac{\int_{\theta_0}^{\theta_f} g(\theta)d\theta - \int_{\theta_f}^{\pi/2} g(\theta)d\theta}{\cos^2\theta_0 - \nu\sin^2\theta_0}\right]_{max} \quad (25)$$

where σ_c^f is the composite strength contributed by short fibres, i.e. the direct short fibre strengthening.

For composites reinforced with unidirectional short fibres, $f(\theta)$ is a delta function at $\theta = 0$. Substituting $f(\theta)$ into Equation 25 yields

$$\sigma_c^f = V_f\sigma_f\left\{1-\frac{\bar{d}}{\bar{l}}[(V_f^{-1/2}-1)E_f/G_m]^{1/2}\right\} \quad (26)$$

For composites reinforced with two-dimensional randomly-oriented short fibres, the fibre-orientation distribution can be expressed as

$$f(\theta) = \frac{2}{\pi} \quad (27)$$

Substituting Equation 27 into Equation 25 yields

$$\sigma_c^f = \frac{V_f\sigma_f}{16\pi}\left\{1-\frac{\bar{d}}{\bar{l}}[(V_f^{-1/2}-1)E_f/G_m]^{1/2}\right\}[B(\theta_0)]_{max} \quad (28)$$

where

$$B(\theta_0) = \left[4(3-\nu)\left(2\theta_f - \frac{\pi}{2} - \theta_0\right) + 16\sin 2\theta_f + 2(1+\nu)\sin 4\theta_f - 8\sin 2\theta_0 - (1+\nu)\sin 4\theta_0\right] \Big/ (\cos^2\theta_0 - \nu\sin^2\theta_0) \quad (29)$$

Calculation shows that for $\nu = 0 - 1.5$, $B(\theta_0)$ reaches its maximum at $\theta_0 = 0$, i.e.

$$[B(\theta_0)]_{max} = B(0) = 4(3-\nu)\left(2\theta_f - \frac{\pi}{2}\right) + 16\sin 2\theta_f + 2(1+\nu)\sin 4\theta_f \quad (30)$$

Substituting Equation 11 into Equation 30 yields

$$[B(\theta_0)]_{max} = 4(3-\nu)\left[2\arcsin\frac{1}{(1+\nu)^{1/2}} - \frac{\pi}{2}\right] + \frac{8\nu^{1/2}(3+\nu)}{1+\nu} \quad (31)$$

Substituting Equation 31 into Equation 28 yields

$$\sigma_c^f = \frac{V_f\sigma_f}{4\pi}\left\{1-\frac{\bar{d}}{\bar{l}}[V_f^{-1/2}-1)E_f/G_m]^{1/2}\right\} \times \left\{(3-\nu)\left[2\arcsin\frac{1}{(1+\nu)^{1/2}} - \frac{\pi}{2}\right] + \frac{2\nu^{1/2}(3+\nu)}{1+\nu}\right\} \quad (32)$$

For composites reinforced with three-dimensional randomly-oriented short fibres, the fibre orientation distribution can be expressed as [12, 13]

$$f(\theta) = \sin\theta \quad (33)$$

Substituting Equations 24 and 33 into Equation 25 and integrating yields

$$\sigma_c^f = V_f\sigma_f\left\{1-\frac{\bar{d}}{\bar{l}}[(V_f^{-1/2}-1)E_f/G_m]^{1/2}\right\}[D(\theta_0)]_{max} \quad (34)$$

where

$$D(\theta_0) = \frac{\nu}{3}(2\cos^3\theta_f - \cos^3\theta_0) - \frac{1+\nu}{5}(2\cos^5\theta_f - \cos^5\theta_0)/(\cos^2\theta_0 - \nu\sin^2\theta_0) \quad (35)$$

Calculation shows that for $\nu = 0 - 1.5$, $D(\theta_0)$ reaches its maximum at $\theta_0 = 0$, i.e.

$$[D(\theta_0)]_{max} = D(0) = \frac{\nu}{3}(2\cos^3\theta_f - 1) - \frac{1+\nu}{5}(2\cos^5\theta_f - 1) \quad (36)$$

Substituting Equations 11 and 36 into Equation 34 yields

$$\sigma_c^f = \frac{V_f\sigma_f}{15}\left\{1-\frac{\bar{d}}{\bar{l}}[V_f^{-1/2}-1)E_f/G_m]^{1/2}\right\} \times \frac{4\nu^{5/2} + (3-2\nu)(1+\nu)^{3/2}}{(1+\nu)^{3/2}} \quad (37)$$

2.2. Residual thermal stress

Metal-matrix and some polymer-matrix composites are generally synthesized at high or intermediate temperatures. Ceramic and glass fibres usually have lower thermal expansion coefficients than metal and polymer matrices, which result in compressive residual thermal stress in fibres during the cooling from the composite synthesis temperature. Assuming that the residual thermal stress in short fibres is σ_t, this stress changes the apparent fibre strength, and makes a positive contribution to the tensile strength of a composite if $\sigma_t < 0$ (compressive stress) but negative contribution if $\sigma_t > 0$ (tensile stress). The contribution of thermal stress to the tensile strength of a composite, σ_c^t, can be calculated from Equation 25 as

$$\sigma_c^t = V_f\sigma_t\left\{1-\frac{\bar{d}}{\bar{l}}[(V_f^{-1/2}-1)E_f/G_m]^{1/2}\right\} \times \left[\frac{\int_{\theta_0}^{\theta_f} g(\theta)d\theta - \int_{\theta_f}^{\pi/2} g(\theta)d\theta}{\cos^2\theta_0 - \nu\sin^2\theta_0}\right]_{max} \quad (38)$$

The magnitude of residual thermal stress in short fibres is sensitive to the composite processing parameters, such as the synthesis temperature and the subsequent cooling rate. It is also related to the fibre and matrix properties such as their thermal expansion

coefficients and diffusivity. The residual thermal stress can be measured by X-ray and neutron diffraction [25].

2.3. Matrix strengthening

For metal-matrix/short-fibre composites, the matrix may be strengthened by high-density thermal stress-induced dislocations [26–28]. The thermal stress is caused by the difference in thermal expansion coefficients between the matrix and the fibre. The matrix strengthening by these thermal stress-induced dislocations can be calculated as [13, 26, 27]

$$\Delta\sigma_{m1} = 2\alpha G_m \boldsymbol{b}\rho_t^{1/2} \quad (39)$$

where $\alpha = 0.3 - 0.5$ is a constant, G_m is the shear modulus of the matrix, $\boldsymbol{b}$ is the Burgers vector and ρ_t is the density of thermal stress-induced dislocations. Dislocations not caused by thermal stress are not considered here because their strengthening effect is usually included in the pure matrix properties during the calculation of composite strength. Another matrix strengthening mechanism is short fibre dispersion hardening, which can be calculated as [13]

$$\Delta\sigma_{m2} = 4G_m\boldsymbol{b}\left\{\bar{d}\left(\frac{\pi}{V_f}\right)^{1/6}\left[\left(\frac{\pi}{V_f}\right)^{1/3} - 6^{1/3}\right]\right\}^{-1} \quad (40)$$

2.4. Composite strength calculation

All the strengthening mechanisms discussed above can be incorporated into the calculation of composite strength

$$\sigma_c = (1 - V_f)\sigma'_m + \sigma_c^t + \sigma_c^f \quad (41)$$

where V_f is the fibre volume fraction, σ'_m is the matrix strength at composite failure, σ_c^t is the residual thermal stress strengthening and σ_c^f is the direct fibre strengthening. For metal matrix composites, σ'_m can be calculated as

$$\sigma'_m = \sigma_m + \Delta\sigma_{m1} + \Delta\sigma_{m2} \quad (42)$$

where σ_m is the calculated matrix stress at composite failure without the consideration of matrix strengthening by thermal stress-induced dislocations and by dispersion hardening.

Substituting Equations 25 and 38 into Equation 41 yields

$$\sigma_c = (1 - V_f)\sigma'_m + V_f\sigma'_f\left\{1 - \frac{\bar{d}}{\bar{l}}[(V_f^{-1/2} - 1)E_f/G_m]^{1/2}\right\} \times \left[\frac{\int_{\theta_0}^{\theta_f} g(\theta)d\theta - \int_{\theta_f}^{\pi/2} g(\theta)d\theta}{\cos^2\theta_0 - \nu\sin^2\theta_0}\right]_{max} \quad (43)$$

where

$$\sigma'_f = \sigma_f - \sigma_t. \quad (44)$$

Accordingly, the strength of unidirectional short fibre composites can be derived from Equations 26 and 41 as

$$\sigma_c = (1 - V_f)\sigma'_m + V_f\sigma'_f\left\{1 - \frac{\bar{d}}{\bar{l}}[(V_f^{-1/2} - 1)E_f/G_m]^{1/2}\right\} \quad (45)$$

σ_c for two-dimensional randomly-oriented short fibre composites can be derived from Equations 32 and 41 as

$$\sigma_c = (1 - V_f)\sigma'_m + \frac{V_f\sigma'_f}{4\pi}\left\{1 - \frac{\bar{d}}{\bar{l}}[(V_f^{-1/2} - 1)E_f/G_m]^{1/2}\right\} \times \left[(3 - \nu)\left[2\arcsin\frac{1}{(1+\nu)^{1/2}} - \frac{\pi}{2}\right] + \frac{2\nu^{1/2}(3+\nu)}{1+\nu}\right] \quad (46)$$

and σ_c for three-dimensional randomly-oriented short fibre composites can be derived from Equation 37 and 41 as

$$\sigma_c = (1 - V_f)\sigma'_m + \frac{V_f\sigma'_f}{15}\left\{1 - \frac{\bar{d}}{\bar{l}}[(V_f^{-1/2} - 1)E_f/G_m]^{1/2}\right\} \times \frac{4\nu^{5/2} + (3 - 2\nu)(1+\nu)^{3/2}}{(1+\nu)^{3/2}} \quad (47)$$

3. Discussion

The strength theory for three-dimensional short fibre composites developed in this paper uses the maximum load criterion for composite failure, which is straight forward and easy to use. Some of the data needed for calculating composite strength, such as the fibre orientation-distribution function, $f(\theta)$, average fibre length, $\bar{l}$, average fibre diameter, $\bar{d}$, and fibre volume fraction, V_f, can either be obtained by image analysis [17], or are known before the fabrication of a composite; some other data, such as metal matrix dispersion hardening, $\Delta\sigma_{m2}$, fibre fracture strength, σ_f, matrix shear modulus, G_m, residual thermal stress, σ_t, and dislocation density, ρ, may be estimated or experimentally determined. However, σ_t and ρ might often need to be estimated because of the experimental difficulty in their determination.

Rearranging Equation 46, we have the following equation for calculating the strength of two-dimensional randomly-oriented short fibre composites

$$\sigma_c = (1 - V_f)\sigma'_m + \frac{\eta V_f\sigma'_f}{4\pi}\left\{(3 - \nu)\left[2\arcsin\frac{1}{(1+\nu)^{1/2}} - \frac{\pi}{2}\right] + \frac{2\nu^{1/2}(3+\nu)}{1+\nu}\right\} \quad (48)$$

where

$$\eta = 1 - \frac{\bar{d}}{\bar{l}}[(V_f^{-1/2} - 1)E_f/G_m]^{1/2} \quad (49)$$

Owing to the lack of experimental data, a comprehensive comparison of the present theory with

experimental results is difficult. Nevertheless, some validation of the present theory can be made with limited available experimental data. Tensile strength data for two-dimensional randomly-oriented E-glass short fibre-reinforced polyethylene-matrix composites have been reported by Lees [29]. Using a Poisson's ratio of $\nu = 0.33$, fibre strength $\sigma_f = 1.95$ GPa [5], and deriving the η values from Lees's work [29], theoretical composite strength can be calculated using Equation 48 (see Fig. 3 for input data). The results are compared with the experimental data in Fig. 3. It can be seen that theoretical composite strength agrees well with the experimental data.

Experimental data exist for aluminium alloy- and pure aluminium-matrix composites reinforced with three-dimensional randomly-oriented alumina short fibres [10]. For example, an Al–7Si matrix composite with 20% δ-alumina fibres has an experimental strength of 237 MPa, and a commercially pure aluminium-matrix composite with 25% δ-alumina fibres has an experimental strength of 175 MPa. Friend's empirical equation [1, 10]

$$\sigma_c^f = \frac{V_f \sigma_f}{5}\left(1 - \frac{l_c}{2l}\right) \quad (50)$$

predicts a strength of 227.2 MPa for the Al–7Si matrix composite, which is reasonably close to the experimental strength of 237 MPa. However, it predicts a strength of only 120 MPa for the commercially pure aluminium-matrix composite, which is 31% lower than the experimental strength. The failure of Friend's equation in predicting the strength of pure aluminium-matrix short fibre composite is probably because it does not consider the matrix work hardening caused by the additional high-density dislocations induced by thermal stress.

Because the thermal stress-induced dislocation density data are not available for the above two composites, we cannot directly calculate their strength using our new theory. However, using the data available, we can calculate the thermal stress-induced dislocation density needed for the composites to have their experimentally observed strengths. Assuming that the residual compressive thermal stress in the alumina short fibres is 35 MPa [20], the thermal stress-induced dislocation density that is needed for the Al–7Si alloy reinforced with 20% alumina fibres to have a strength of 237 MPa is 2.78×10^8 cm^{-2}; and the thermal stress-induced dislocation density that is needed for the pure aluminium reinforced with 25% alumina fibres to have a strength of 175 MPa is 5.9×10^9 cm^{-2}. It can be seen that the calculated thermal stress-induced dislocation density is higher in the pure aluminium matrix. This is reasonable, in that the pure aluminium has lower yielding stress than aluminium alloys, thus making it easier for dislocations to form and multiply. No experimental data are available to compare with the above calculated dislocation density. However, experimental data in a similar composite system have been reported [20, 30]. It is observed that the dislocation density around fibres in a SiC short fibre-reinforced aluminium alloy matrix

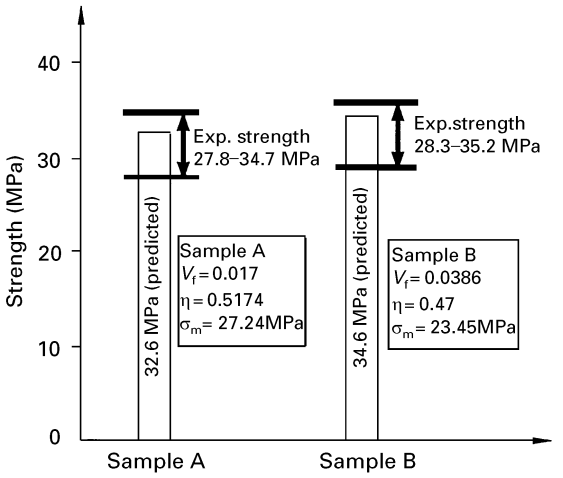

Figure 3 The theoretical strengths calculated using Equation 48 show good agreement with the experimental strength data of two-dimensional randomly-oriented E-glass short fibre-reinforced polyethylene-matrix composites.

composite is 10^9 to 4×10^{10} cm^{-2}, and in the matrix away from SiC fibres, the dislocation density is much lower [20, 30]. The average thermal stress-induced dislocation density over the entire aluminium alloy matrix should be much lower than the above observed values, and our calculated thermal stress-induced dislocation density values are reasonable.

The present theory can also be used to analyse contributions of various strengthening mechanisms to the composite strength. For example, an Al–12Si matrix composite reinforced with 25% three-dimensional randomly-oriented alumina short fibres has been reported to have a strength of 162.63 MPa. Calculation using the present theory shows that the contribution of direct fibre strengthening is 83.33 MPa, which is 51% of the composite strength; the contribution of residual thermal stress (assuming 35 MPa compressive stress in short fibres) is 1.46 MPa (1% of the composite strength); the contribution of fibre dispersion-hardening is 8.51 MPa (5% of the composite strength); the contribution of unstrengthened matrix is 63.95 MPa (39% of the composite strength); and the contribution of thermal stress-induced dislocation hardening is 5.38 MPa (3% of the composite strength). This analysis gives us some insight into the composite strengthening mechanisms and is useful in composite strength assessment and design.

4. Conclusion

The theory developed in this paper for calculating the tensile strength of three-dimensional oriented short-fibre composite improves upon previous strength theories. The present theory can take into account some material parameters which have not been comprehensively considered by previous theories, such as the short fibre-orientation distribution, matrix shear modulus, residual thermal stress in short fibres, and dispersion hardening and thermal stress-induced dislocation hardening in a metal matrix. It adopts a maximum-load composite failure criterion in calculating

the direct contribution of short fibres toward the composite strength, which is straight forward and easy to use. Comparison with the experimental data of two-dimensional randomly-oriented short fibre-reinforced polyethylene-matrix composite shows good agreement. The contribution of various strengthening mechanisms towards the composite strength can also be estimated using the present theory, providing useful information for composite design.

Acknowledgements

The authors acknowledge the support provided by the Director's Postdoctoral Fellowship and the Laboratory Directed Research and Development Office of Los Alamos National Laboratory. This work was performed at Los Alamos National Laboratory under the auspices of the US Department of Energy (contract W-7405-EN-36).

References

1. M. M. SCHWARTZ, "Composite Materials Handbook", 2nd edn (McGraw-Hill, New York, 1992) Ch. 7, pp. 54–61.
2. D. J. BAY, in "Composite Applications", edited by T. J. Drozda (Society of Manufacture Engineers, Dearborn, MI, 1989) pp. 3–23.
3. B. W. ROSEN, "Fiber Composite Materials" (American Society for Metals, Metals Park, OH, 1964) p. 37.
4. Y. T. ZHU, B. L. ZHOU, G. H. HE and Z. G. ZHENG, *J. Compos. Mater.* **23** (1989) 280.
5. D. HULL, "An Introduction to Composite Materials" (Cambridge University Press, London, 1981) pp. 14 and 200.
6. Z. GAO, K. L. REIFSNIDER and G. CARMAN, *J. Compos. Mater.* **26** (1992) 1678.
7. Y. T. ZHU and G. ZONG, *ibid.* **27** (1993) 944.
8. P. E. CHEN, *Polym. Eng. Sci.* **11** (1971) 51.
9. J. C. HALPIN and J. L. KARDOS, *ibid.* **18** (1978) 496.
10. C. M. FRIEND, *J. Mater. Sci.* **22** (1987) 3005.
11. *Idem*, *Scripta Metall.* **23** (1989) 33.
12. H. FUKUDA, T. W. CHOU and K. KAWATA, in "Proceedings of Japan-US Conference on Composite Materials: Mechanics, Mechanical Properties and Fabrication", edited by K. Kawata and T. Akasaka (Applied Science Publisher, The Japan Society for Composite Materials, Tokyo, 1982) p. 181.
13. Y. T. ZHU, G. ZONG, A. MANTHIRAM and Z. ELIEZER, *J. Mater. Sci.* **29** (1994) 6281.
14. Y. T. ZHU and W. R. BLUMENTHAL, in "Micromechanics of Advanced Materials", edited by S. N. G. Chu, P. K. Liaw, R. J. Arsenault, K. Sadananda, K. S. Chen, W. W. Gerberich, C. C. Chau and T. M. Kung (The Minerals, Metals and Materials Society, Warrendale, PA, 1995) pp. 481–85.
15. S. H. McGEE and R. L. McCULLOUGH, *J. Appl. Phys.* **55** (1984) 1394.
16. G. FISHER and P. EYERE, *Polym. Compos.* **9** (1988) 297.
17. Y. T. ZHU, W. R. BLUMENTHAL and T. C. LOWE, *J. Comp. Mater.*, in press.
18. L. M. GONZALEZ, F. L. CUMBRERA, F. SANCHEZ-BAJO and A. PAJARES, *Acta Metall. Mater.* **42** (1994) 689.
19. R. W. HERTZBERG, "Deformation and fracture mechanics of Engineering Materials" (Wiley, New York, 1989) p. 136.
20. R. J. ARSENAULT and R. M. FISHER, *Scripta Metall.* **17** (1983) 67.
21. N. SHI, B. WILNER and R. J. ARSENAULT, *Acta Metall. Mater.* **40** (1992) 2841.
22. R. J. ARSENAULT and N. SHI, *Mater. Sci. Eng.* **81** (1986) 175.
23. L. F. SMITH, A. D. KRAWITZ, P. CLARKE, S. SAIMOTO, N. SHI and R. J. ARSENAULT, *ibid.* **A159** (1992) L13.
24. B. W. ROSEN, *AIAA J.* **2** (1964) 1985.
25. I. C. NOYAN, "Residual Stress" (Springer, New York, 1987) p. 6.
26. S. M. PICKARD, S. SCHMAUDER, D. B. ZAHL and A. G. EVANS, *Acta Metall. Mater.* **40** (1992) 3113.
27. D. C. DUNAND and A. MORTENSEN, *ibid.* **39** (1991) 127.
28. C. Y. BARLOW and N. HANSEN, *ibid.* **39** (1991) 1971.
29. J. K. LEES, *Polym. Eng. Sci.* **8** (1968) 195.
30. C. T. KIM, J. K. LEE and M. R. PLICHTA, *Metall. Trans.* **21A** (1990) 673.

Received 6 February
and accepted 17 September 1996